Collective electronic excitations and their damping in small alkali clusters

Yang Wang [a,b], Caio Lewenkopf [a,c], David Tománek [a,b], George Bertsch [a,c,1]

[a] *Department of Physics and Astronomy, Michigan State University, East Lansing, MI 48824-1116, USA*
[b] *Center for Fundamental Materials Research, Michigan State University, East Lansing, MI 48824-1116, USA*
[c] *National Superconducting Cyclotron Laboratory, Michigan State University, East Lansing, MI 48824-1116, USA*

and

Susumu Saito

Fundamental Research Laboratories, NEC Corporation, 34 Miyukigaoka, Tsukuba, Ibaraki 305, Japan

We calculate collective electronic excitations and their damping in small Na_n and Li_n clusters. The ground state properties of these systems are described using the local density approximation, and the electronic excitations by the random phase approximation. The collective excitations in the first two closed-shell clusters with $n = 2, 8$ atoms are discussed in detail. We find that the coupling of electronic levels to vibrational degrees of freedom accounts quantitatively for the observed width of the collective electronic excitations in alkali dimers. The origin of the analogous line broadening in Na_8 is presently unresolved.

Alkali-metal clusters are very interesting systems which bridge the gap between isolated atoms and bulk metals. The large degree of delocalization of valence electrons, characteristic of the simple metals, is an important property of these clusters. This delocalization shows up most dramatically in the appearance of magic numbers corresponding to shell orbitals encompassing the entire cluster [1,2]. The electronic response of these systems is particularly interesting in that it shows one of the characteristics of a macroscopic plasmon, namely a large fraction of the oscillator strength concentrated in a narrow frequency range [3]. In the following, we will address this collective mode as the cluster plasmon mode [3]. In contrast to the prediction of the classical Mie theory as applied to metal spheres, this collective mode is typically 30% lower in frequency for small clusters, and does show a pronounced size dependence [4].

Moreover, the discrepancy between the classical Mie picture and the observed excitation energy is much larger in Li_n than in Na_n clusters, for reasons presently unknown [5].

Of especial interest to us is the width of the collective excitation. The observed width of the plasmon peak is 0.11 eV in Na_2 [6] and 0.25 eV in Na_8 [7], much larger than the natural line width for the photoexcitation. In large clusters with a high density of states near the highest occupied (HOMO) and lowest unoccupied molecular orbital (LUMO), particle–hole excitations (Landau damping) and multiparticle–hole excitations will dominate the fragmentation of the plasmon [8,9]. In the small clusters with $n \lesssim 8$–40 atoms, however, Landau damping is considered to be negligible due to the low level density near the HOMO. As we will show below, the dominant plasmon damping mechanism in these systems results from the coupling of electronic excitations to cluster vibrations. The quantum motion of nuclei gives a broadening which is described more precisely as a distribution of states with a variable

number of vibrational quanta excited together with the plasmon. An increased nuclear motion in the ground state has been estimated to account for a line broadening with increasing temperature [10,11].

Because of the large number of vibrational modes and the small value of the vibrational energy, it hardly makes sense to study this effect by explicit calculation of the vibrational wave functions and the associated Franck-Condon factors for the transitions. Instead, we shall apply an approximation that directly gives the width of the strength distribution irrespective of the quantization of the vibrational final state.

We determine the ground state structural and electronic properties of small alkali clusters using the local density approximation (LDA) [12]. Electronic excitations are calculated using the random phase approximation (RPA) [13], using LDA single-particle wave functions and energies. In this Letter, we apply this formalism to Li_2, Na_2 and Li_8, Na_8 clusters. The complete spectroscopy of the dimers is well established [14]. Consequently, these systems are ideally suitable for testing the accuracy of our methods in the ground state, and the power of our predictions in the excited state. For the larger clusters, the scenario is not so clear, since even their exact ground state geometry is uncertain [15-18]. We proceed as follows. We first demonstrate the precision of our method by calculating the ground state properties of the bulk metals and comparing them to experimental data. We do the same for the ground state of the addressed clusters. Next, we use the LDA-RPA to determine the excitation spectra. Finally, we determine the coupling of electronic excitations to cluster vibrations and compare the results with experiment.

In our LDA calculations, we consider the valence electrons only, and describe the effect of the core electrons by ab initio norm-conserving nonlocal pseudopotentials. Our pseudopotentials have been generated using the Hamann-Schlüter-Chiang scheme [19]. The electronic configurations which we used to generate the pseudopotentials, Li $2s^{0.8}2p^{0.1}$ (with the core radii $r_c(2s) = 0.915$ Å and $r_c(2p) = 0.788$ Å) and Na $3s^{0.7}3p^{0.1}3d^{0.05}$ ($r_c(3s) = 1.005$ Å, $r_c(3p) = 1.323$ Å, $r_c(3d) = 1.746$ Å), provide very good transferability especially towards the excited states. A partial core correction has been used

in the LDA calculations [20]. We use the Ceperley-Alder parametrization of the exchange-correlation potential [21] in the Kohn-Sham equations.

In order to minimize the influence of a finite basis on our results, we decide to place our clusters on a face-centered cubic superlattice with a large lattice constant. This minimizes the volume associated with each cluster for a constant inter-cluster separation. Plane waves are the natural basis in the case which can be improved systematically. We find this approach more reliable for alkali clusters with delocalized electron states than an atom-centered Gaussian basis. Treament of an isolated cluster in real space on a radial grid turns out numerically as involved as our approach. We used an energy cutoff in the Fourier expansion of the charge density $E_{max} = 6.9$ Ry for the solid and $E_{max} = 4.0$ Ry for the clusters. Symmetry has been used to reduce the computational effort. The lattice constant $a = 15$ Å for the superlattice guarantees negligible overlap between the clusters and hence vanishing crystal field splitting, as verified by comparing the band structure at different points in the (very small) Brillouin zone.

The calculated ground state properties of bulk Li are the lattice constant $a_{LDA} = 3.42$ Å ($a_{exp} = 3.49$ Å [22]), the bulk cohesive energy (with respect to an isolated spin-polarized atom) $E^{coh}_{LDA} = 1.64$ eV ($E^{coh}_{exp} = 1.63$ eV [22]), and the bulk modulus $B_{LDA} = 0.112 \times 10^{11}$ Pa ($B_{exp} = 0.116 \times 10^{11}$ Pa [22]). The corresponding values for Na are $a_{LDA} = 4.04$ Å ($a_{exp} = 4.23$ Å [22]), $E^{coh}_{LDA} = 1.23$ eV ($E^{coh}_{exp} = 1.11$ eV [22]), and $B_{LDA} = 0.089 \times 10^{11}$ Pa ($B_{exp} = 0.068 \times 10^{11}$ Pa [22]). As expected from converged LDA calculations, the bulk is somewhat overbound. The larger difference between the calculated and the observed bulk moduli is presumably due to the pseudopotential approximation which suppresses exchange and correlation between valence and core orbitals. This effect is expected to be much smaller in atomic clusters where long-range exchange and correlation is absent.

The smallest system we aim to describe are the dimers, the first closed-shell system within the spherical jellium background model. The large stability of alkali dimers is explained within the jellium model by a large separation between the fully occupied 1s state and the empty 1p state of the cluster. The dimer geometry deforms the charge density along the mo-
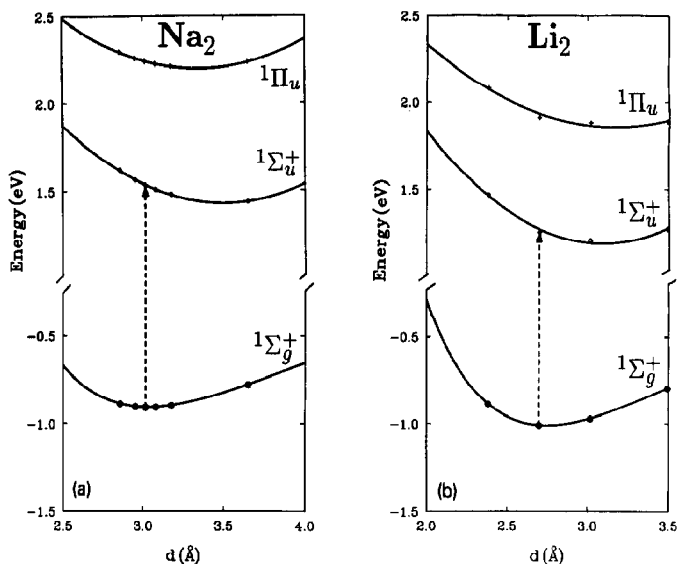
Fig. 1. Franck–Condon broadening of the collective electronic excitations in (a) Na_2 and (b) Li_2. The lowest levels are the LDA dissociation energies $D(d)$ of the dimers as a function of the bond length d. The higher levels give the excitation energies, which are presented as $D(d) + E_{RPA}(d)$.

Table 1
Ground state properties of sodium and lithium dimers. Equilibrium bond length d_e, dissociation energy D_e, and vibration frequency ω_e

System	d_e (Å)		D_e (eV)		$\hbar\omega_e$ (meV)	
	exp. [a]	theory	exp. [a]	theory	exp. [a]	theory
Li_2	2.672	2.730	1.03	1.01	43.572	46.0
Na_2	3.078	3.032	0.72	0.91	19.742	20.0

[a] See ref. [14].

lecular axis, and splits the threefold degenerate 1p level into one σ and two π states. The dimer has only one nuclear degree of freedom, the dimer stretch mode, which simplifies the calculation of electron-vibration coupling significantly.

In fig. 1, we show the total energy of the system as a function of the interatomic distance. LDA results for dissociation energies, bond lengths and vibrational energies of Li_2 and Na_2, shown in table 1, are in striking agreement with the experimental values [14].

The next closed-shell configuration in alkali clusters occurs for eight atoms. The physics of these systems is much more complex due to their eighteen nuclear degrees of freedom and many different isomers

which lie close in energy. As mentioned before, not even the equilibrium geometry is well established [15–18], although calculations [16–18] suggest the T_d symmetry for the ground state. Consequently, we base our calculations on this geometry. The LDA superlattice calculations are essentially the same as for the dimers, but we increase the fcc lattice constant to $a = 50$ Å in order to minimize the interaction between clusters. The latter was checked by observing the calculated band dispersion $\Delta\epsilon$ across the Brillouin zone. Our value $\Delta\epsilon \approx 0.01$ eV, gives an estimate for the upper bound of cluster–cluster interaction. We use again an energy cutoff of 4.0 Ry, corresponding to a plane wave basis with 4279 components. The equilibrium structure of these clusters in the T_d ge-

ometry is uniquely defined by the radial distance d_i of the "inner tetrahedron" atoms from the cluster center, and the corresponding distance d_o of the outer tetrahedron atoms. The calculated atomization energy per atom for the Na_8 cluster in equilibrium geometry with $d_i = 2.11$ Å and $d_o = 3.51$ Å is 0.77 eV, in reasonable agreement with the value of 0.86 eV, obtained in a previous LSDA calculation [15].

Once the equilibrium geometries are known, we proceed to calculate the response to external electric fields. The static response is a ground state property of the system and can be obtained directly from LDA. We use the above described superlattice geometry [*1] to determine the static dielectric response of these systems to a field which is parallel or perpendicular to the dimer axis. For an isolated Na atom we find $\alpha_{LDA}(Na) = 22.0$ Å^3, in good agreement with the experimental value of $\alpha_{exp}(Na) = 23.6$ Å^3 [23]. The polarizability of a negatively charged sodium ion $\alpha_{LDA}(Na^-)$ is 63.0 Å^3, much larger than that of the atom, caused by the weak binding of the outermost electron. The polarizability of the Na_2 along the axis is $\alpha_{LDA}^{\parallel}(Na_2) = 63.5$ Å^3, while the value perpendicular to the axis is $\alpha_{LDA}^{\perp}(Na_2) = 22.1$ Å^3. The average over all directions of the polarizability gives $\langle \alpha_{LDA}(Na_2) \rangle = \frac{1}{3}\sum_{i=1}^{3} \alpha_i = 35.9$ Å^3, which can be measured experimentally. This values agrees well with local spin density approximation (LSDA) calculations of Moullet et al. [18], who obtained $\alpha^{\parallel}(Na_2) = 53$ Å^3 and $\alpha^{\perp}(Na_2) = 30$ Å^3, leading to $\langle \alpha_{LDA}(Na_2) \rangle = 37.7$ Å^3.

Once the static dielectric response is established, we proceed to calculate the electronic excitation spectrum within the linear response framework. We use the RPA which is based on an electronic ground state described by LDA. RPA automatically satisfies energy-weighted sum rules, and has the correct physical limits, namely independent-particle transitions at high momentum transfer, where the interaction is weak, and strong collective excitations at low momentum transfer, where the interaction is strong. It is customary in condensed matter physics to imple-

ment RPA by choosing the potential field as the basic object of computation. In this case, the wave function enters indirectly via the dynamic polarizability. However, if only a few electron states participate in the excitation, the most efficient approach is to set up the RPA equations for the wave function directly [24]. We shall use this method in the present work.

We start with the single-electron wave functions $\phi_i(r)$ and energies ϵ_i, obtained from the LDA calculation. We shall need both occupied and unoccupied orbitals, from which we construct the particle–hole states. We designate the particle–hole state as $|ij^{-1}\rangle$, where i designates an unoccupied (particle) state and j an occupied (hole) state. The Hamiltonian matrix may be separated into a diagonal part that gives the energy of the particle–hole state, and an off-diagonal part that describes the coupling to other particle–hole excitations. The diagonal part includes the kinetic energy operator and the self-consistent Hartree field. We write this part of the Hamiltonian matrix as

$$\langle ij^{-1} | \epsilon | i'j'^{-1} \rangle = \delta_{ii'}\delta_{jj'}(\epsilon_i - \epsilon_j) . \tag{1}$$

The residual interaction contributes matrix elements of the form

$$\langle ij^{-1} | v | i'j'^{-1} \rangle$$
$$= \int dr\, dr'\, \phi_i^*(r)\phi_j(r')v(r,r')\phi_{i'}(r)\phi_{j'}^*(r'), \tag{2}$$

where v includes the residual Coulomb interaction and exchange correlation. The RPA eigenvectors u^α and their associated frequencies ω_α are given by the eigenvalue equation

$$(\hbar\omega_\alpha)^2 u^\alpha = \epsilon^{1/2}(\epsilon + 2v)\epsilon^{1/2}u^\alpha . \tag{3}$$

Here, the vector and matrix indices have been omitted for simplicity, and u_{ij}^α represents the amplitude of the particle–hole configuration $|ij^{-1}\rangle$ in the collective mode α. The normalization of the amplitudes is given by $\sum_{ij}|u_{ij}^\alpha|^2 = 1/\hbar\omega_\alpha$. Finally, the transition strength with an external field $D(r)$ is given by $|\langle \alpha | D | 0 \rangle|^2 = |\sum_{ij} u_{ij}^\alpha \langle i | D | j \rangle|^2$.

Let us first discuss the application of the above formalism to the dimers, Li_2 and Na_2. The results of our calculations for these systems, obtained using different approximations, are summarized in fig. 1 and table 2. In fig. 1, we plot the energy of the dimers

---

[*1] In a cluster superlattice, the external field is generally modified by the field of the induced dipoles on the other sites. Since our system has inversion symmetry, the corresponding correction vanishes exactly at each lattice point, and is very small over the cluster volume. The polarizabilities of atoms and dimers can then be obtained directly using second order perturbation theory.
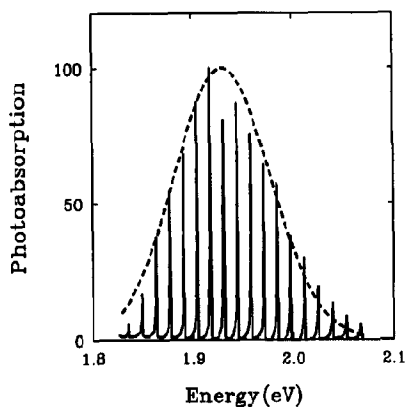
Fig. 2. Calculated spectral function of Na_2 (in arbitrary units) and its broadening due to nuclear zero-point motion (- - -), as compared to the observed photoionization spectrum of ref. [6] (——). The displayed theoretical data are red-shifted by 0.5 eV with respect to the calculated results.

for a given electronic configuration as a function of the bond length d. The lowest curve gives LDA results for the $^1\Sigma_g^+$ ground state. The $^1\Sigma_u^+$ curve is obtained by adding the RPA excitation energy to the energy of the $^1\Sigma_g^+$ state. In the adiabatic approximation, we determine the transitions from the energy difference between the vibrational ground state and the excited state in the same geometry, as indicated by arrows in fig. 1. From fig. 1 we notice that the potential energy surface and equilibrium geometry of the excited state are different from those of the ground state. The equilibrium bond length $d_{e,RPA}^*(Na_2) = 3.50$ Å compares well with the experimental value $d_{e,exp}^*(Na_2) = 3.63$ Å [14]. The corresponding value for Li_2 is $d_{e,RPA}^*(Li_2) = 3.17$ Å,

which again compares well with the observed value $d_{e,exp}^*(Li_2) = 3.10$ Å [14]. Experimental data [14] indicate that the energy difference between the $^1\Sigma_g^+$ ground state at d_e and the $^1\Sigma_u^+$ excited state at d_e^* is 1.76 eV for Li_2 and 1.82 eV for Na_2. These energies compare reasonably well with our LDA–RPA results of 2.20 eV for Li_2 and 2.33 eV for Na_2. However, a comparison between calculated and observed adiabatic (vertical) excitation energies in table 2 shows that the calculated plasmon energy is blue-shifted by 0.5 eV (see fig. 2) with respect to the observed value. This blue-shift is characteristic of LDA–RPA calculations, and reflects the incorrect asymptotic behavior of the effective potential.

As we will discuss below, the difference between the potential energy surfaces in the ground and the excited state is responsible for vibrational broadening of electronic excitations. Of particular importance in this respect is the shape of the excited potential energy surface. We find our calculated values for the vibrational frequencies in the $^1\Sigma_u^+$ state $\omega_e^*(Li_2) = 31.7$ meV and $\omega_e^*(Na_2) = 17.8$ meV to compare very well with the experimental data [14] $\omega_{e,exp}^*(Li_2) = 31.7$ meV and $\omega_{e,exp}^*(Na_2) = 14.6$ meV.

As expected and discussed in the following, these results are superior to calculations for spherical jellium representing Na_2 and Li_2 clusters. Our corresponding LDA–RPA results, obtained using the JELLY-RPA program [25], are shown in table 2. In the jellium model scenario, the *single-particle* ground state has a 1s character, and the lowest unoccupied states have 1p, 1d and the 2s character. The spherical potential clearly cannot describe the splitting of the first two excited states which is substantial in the dimers. Among the above jellium states, there is only

Table 2

Collective electronic excitations in small sodium and lithium clusters. Our results for the plasmon frequency $\hbar\omega_{plasmon}$ and its width Γ are listed together with results based on spherical jellium [25], $\hbar\omega_{JELLY-RPA}$, and results of the classical Mie theory, $\hbar\omega_{Mie}$

System	$\hbar\omega_{plasmon}$ (eV)		Γ (eV)		$\hbar\omega_{JELLY-RPA}$ (eV) theory	$\hbar\omega_{Mie}$ (eV) theory
	exp.	theory	exp.	theory		
Li_2	1.76 [a,b]	2.23	0.06 [a,b]	0.063	3.6	4.6
Na_2	1.92 [c]	2.43	0.11 [c]	0.095	2.8	3.5
Li_8	2.55 [b]		0.4 [b]		3.6	4.6
Na_8	2.53 [d]	3.10	0.25 [d]	0.03	2.8	3.5

[a] See ref. [26].   [b] See ref. [27].   [c] See ref. [6].   [d] See ref. [7].

one dipole-allowed transition from the ground state, namely the 1s→1p transition. Other allowed transitions have a much larger excitation energy, and are essentially single-particle transitions. Our numerical results, shown in table 2, yield values for the collective excitations in jellium which lie up to 60% above the LDA–RPA results for the realistic geometry, mainly due to the spherical approximation in the jellium model. Another important disadvantage of spherical jellium is that it cannot address vibrational damping of electronic excitations, which we shall discuss below.

Next, we turn to the Li_8 and Na_8 clusters. The results for the collective excitation energies in these systems, obtained using different approximations, are summarized in table 2. The LDA calculation for spherical jellium gives the occupied ground state levels at $\epsilon(1s) = -4.46$ eV and $\epsilon(1p) = -3.19$ eV. The lowest unoccupied states lie at $\epsilon(1d) = -1.65$ eV and $\epsilon(2s) = -1.15$ eV. The relatively large HOMO–LUMO gap of 1.54 eV contributes substantially to the stabilization of this magic cluster size. The LDA–RPA calculations for this system predict a plasmon energy of $\hbar\omega_{JELLY\text{-}RPA} = 2.8$ eV.

Our LDA calculation for Na_8 in T_d geometry shows that the lowest nondegenerate unoccupied level, corresponding to the jellium 2s level, lies at $\epsilon = -0.82$ eV and is lower in energy than the manifold of levels originating from the jellium 1d level. This manifold results from symmetry breaking of the fivefold degenerate 1d type level of the spherical jellium into a threefold degenerate level at $\epsilon = -0.73$ eV (consisting of orbitals with xy, yz, zx character) and a doubly degenerate level at $\epsilon = -0.35$ eV (consisting of orbitals with $2z^2 - x^2 - y^2$, $x^2 - y^2$ character).

The RPA spectrum of Na_8 in the realistic geometry discussed above is given in fig. 3. The spectrum shows three distinct peaks, but is dominated by a single resonance at $\hbar\omega_{plasmon} = 3.1$ eV. This is in agreement with experimental results [7], but disagrees with previously calculated photoabsorption spectra [28]. The strong resonance exhausts 87.4% of the f-sum rule, which is indicative of its strong collective character. As in Na_2, this value is blue-shifted with respect to the experimental value $\hbar\omega_{plasmon,exp} = 2.53$ eV [7].

Our above results indicate that the present scheme is able to determine collective electronic excitation
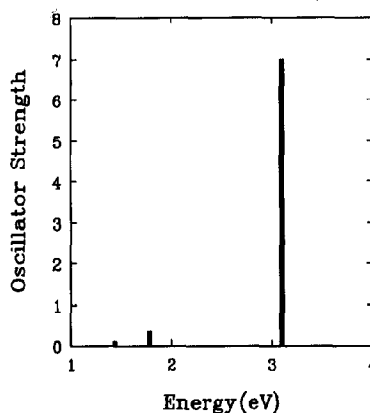
Fig. 3. Calculated oscillator strength distribution in the excitation spectrum of Na_8.

quite well, especially when compared to the jellium model. Equally important as the plasmon excitation energy is the fragmentation of this collective mode. Due to the low level density near the HOMO, Landau damping is improbable in these systems [9]. The dominant broadening mechanism at $T = 0$ K is the coupling of the electronic excitations to nuclear zero-point motion, as described by the Franck–Condon effect. With increasing temperature, higher vibration modes and possibly transformations between different isomers are likely to further broaden the plasmon line width. This thermal broadening mechanism is expected to play a more pronounced role in the larger $n = 8$ atom clusters with soft vibrational modes.

The Hamiltonian which describes the coupling between the electronic excited state ϵ_c and the vibrational normal modes μ with energy $\hbar\omega_\mu$ is [29]

$$H = c^\dagger c\left(\epsilon_c + \sum_\mu M_\mu(a_\mu^\dagger + a_\mu)\right)$$
$$+ \sum_\mu \hbar\omega_\mu a_\mu^\dagger a_\mu. \qquad (4)$$

Here, $c^\dagger$ and $a^\dagger$ are the creation operators for electronic and vibrational states, respectively. In the case of dimers, eq. (4) is strongly simplified due to the presence of a single ground state vibration mode with energy $\hbar\omega_0$. The coupling of electrons to nuclear motion is described by the term $M(a^\dagger + a) \equiv Fx$, where F is the slope of the potential energy surface for the excited state at the transition point. As a result, the

exact solution for the spectral density distribution $A(\hbar\omega)$ at zero temperature is given by the Poisson distribution [29]

$$A(\hbar\omega) = 2\pi e^{-g} \sum_{n=0}^{\infty} \frac{g^n}{n!}$$

$$\delta(\hbar\omega - \epsilon_c + g\hbar\omega_0 - \hbar\omega_1 n) , \qquad (5)$$

where ω_1 is the vibrational frequency of the excited state. In this equation, g is related to the slope F and the ground state vibration energy $\hbar\omega_0$ by $g = F^2/2m\hbar\omega_0^3$, and n gives the corresponding quantum level. $A(\hbar\omega)$ is hence a sum of equally spaced delta functions (as shown in fig. 2), with separation energy $\hbar\omega_0$ and a Poisson peak height distribution. In the limit of large g, the Poisson distribution can be approximated by a Gaussian distribution, as

$$A(\hbar\omega) = \sum_{n=0}^{\infty} \frac{1}{\sqrt{2\pi n}} \exp[-(n-g)^2/2n]$$

$$\times \delta(\hbar\omega - \epsilon_c + g\hbar\omega_0 - \hbar\omega_1 n) . \qquad (6)$$

The resulting line shape has a full width at half maximum (fwhm) Γ, which is given by

$$\Gamma = 2F\sqrt{\frac{\hbar \ln 2}{m\omega_0}} \qquad (7)$$

for the vibrational ground state corresponding to $T = 0$ K. An intuitive way to understand this formula is the following. The probability distribution for a harmonic oscillator in the ground state is a Gaussian with a width $(\Delta x)^2 = \hbar/m\omega_0$. Assuming that the dependency of the excitation energy on x is given by $\Delta E = F\Delta x$, one obtains for the distribution of excitation energies $f(E) = \exp[-m\omega_0(E-E_0)^2/\hbar F^2]$. This is essentially the same result as in eq. (7).

Our results for the plasmon damping in Na_2 and Li_2 are summarized in table 2 and fig. 2. For Li_2, line broadening can be estimated using precise data for the equilibrium geometry and vibrational modes of the ground and the excited states [26]. The corresponding results are given in table 2. For Na_2, we obtain for the $^1\Sigma_g^+ \rightarrow {}^1\Sigma_u^+$ transition a fwhm of 0.10 eV, in very good agreement with the experimental value $\Gamma = 0.11$ eV [6]. The perfect agreement of the envelope functions in fig. 2 indicates that in this case, the coupling between electronic and vibrational de-

grees of freedom dominates the plasmon fragmentation. For the $^1\Sigma_g^+ \rightarrow {}^1\Pi_u$ transition, we predict a line width of 0.06 eV. No experimental data for the line width are presently available for this transition.

Investigations of the vibrational broadening of collective electronic excitations are in progress for Li_8 and Na_8. The calculation is more complex not only due to the larger cluster size, but also due to the significantly larger number of nuclear degrees of freedom in these systems. In order to obtain a rough estimate of the plasmon line broadening in these systems, we proceed as follows. We assume that the broadening is dominated by a single low-frequency mode with a large quadrupolar component. We restrict our calculations of the clusters with assumed T_d geometry to the lowest vibration mode with D_{2d} symmetry, which is obtained using the parametrized many-body alloy Hamiltonian [30]. The LDA–RPA calculation for this distortion indicates only a very small line broadening in Na_8 of $\Gamma \approx 0.03$ eV, much smaller than the observed value $\Gamma_{exp} = 0.25$ eV [7]. The discrepancy between the calculated and the observed value may be due to our neglect of the other vibrational degrees of freedom, or a large temperature of the observed clusters. For a thermally excited cluster, Γ can be estimated in analogy to ref. [11] as $\Gamma = F(k_B T 8 \ln 2/m\omega_0^2)^{1/2}$. Using this expression, and relying on the validity of the harmonic approximation, we find a line broadening of 0.25 eV to correspond to a temperature $T \approx 2000$ K for the vibrational mode above. Even though this temperature is likely to be overestimated by the harmonic approximation, our result suggests that other vibrational modes contribute significantly to the line broadening. Moreover, substantial line broadening could result from structural transitions between different isomers of the $n = 8$ atom structures which are very close in energy [15–18].

In conclusion, we have calculated the equilibrium structure and collective electronic excitations and their damping in small Na_n and Li_n clusters. We have used the local density approximation to describe the ground state properties of these systems, and the random phase approximation for the electronic excitations. We have discussed the collective excitations in the first two closed-shell clusters with $n = 2$, 8 atoms in detail. Our results indicate that the coupling of electronic levels to vibrational degrees of

freedom accounts quantitatively for the observed width of the collective electronic excitations in alkali dimers. More calculations are necessary to address the damping mechanism of the collective electronic excitations in Li_8 and Na_8.

References

[1] W. de Heer, W. Knight, M. Chou and M. Cohen, Solid State Phys. 40 (1987) 93.

[2] S. Bjornholm, J. Borggreen, O. Echt, K. Hansen, J. Pedersen and H.D. Rasmussen, Phys. Rev. Letters 65 (1990) 1627.

[3] W.A. de Heer, K. Selby, V. Kresin, J. Masui, M. Vollmer, A. Chatelain and W.D. Knight, Phys. Rev. Letters 59 (1987) 1805.

[4] J.H. Parks and S.A. McDonald, Phys. Rev. Letters 62 (1989) 2301.

[5] C. Bréchignac, private communication.

[6] A. Herrmann, S. Leutwyler, E. Schumacher and L. Wöste, Chem. Phys. Letters 52 (1977) 418.

[7] C.R.C. Wang, S. Pollack and M.M. Kappes, Chem. Phys. Letters 166 (1990) 26.

[8] C. Yannouleas, R. Broglia, M. Brack and P. Bortignon, Phys. Rev. Letters 63 (1989) 255.

[9] S. Saito, G. Bertsch and D. Tománek, Phys. Rev. B 43 (1991) 6804.

[10] J.M. Pacheco and R.A. Broglia, Phys. Rev. Letters 62 (1989) 1400.

[11] G. Bertsch and D. Tománek, Phys. Rev. B 40 (1989) 2749.

[12] P. Hohenberg and W. Kohn, Phys. Rev. B 136 (1964) 864; W. Kohn and L.J. Sham, Phys. Rev. A 140 (1965) 1133.

[13] D. Bohm and D. Pines, Phys. Rev. 92 (1953) 609.

[14] G. Herzberg, Molecular spectra and molecular structure. Vol. 1. Spectra of diatomic molecules, 2nd Ed. (Van Nostrand, Princeton, 1950).

[15] J.L. Martins, J. Buttet and R. Car, Phys. Rev. B 31 (1985) 1804.

[16] I. Boustani, W. Pewestorf, P. Fantucci, V. Bonačić-Koutecký and J. Koutecký, Phys. Rev. B 35 (1987) 9437.

[17] V. Bonačić-Koutecký, P. Fantucci and J. Koutecký, Phys. Rev. B 37 (1988) 4369.

[18] I. Moullet, J.L. Martins, F. Reuse and J. Buttet, Phys. Rev. Letters 65 (1990) 476.

[19] D.R. Hamann, M. Schlüter and C. Chiang, Phys. Rev. Letters 43 (1979) 1494.

[20] S.G. Louie, S. Froyen and M.L. Cohen, Phys. Rev. B 26 (1982) 1738.

[21] D.M. Ceperley and B.J. Alder, Phys. Rev. Letters 45 (1980) 566; J.P. Perdew and A. Zunger, Phys. Rev. B 23 (1981) 5048.

[22] C. Kittel, Introduction to solid state physics, 6th Ed. (Wiley, New York, 1986).

[23] B. Bederson and D.R. Bates, eds., Advances in atomic and molecular physics, Vol. 13 (Academic Press, New York, 1977).

[24] D.J. Rowe, Nuclear collective motion: models and theory, 1st Ed. (Methuen, London, 1970) ch. 14.

[25] G.F. Bertsch, Comput. Phys. Commun. 60 (1990) 247.

[26] P. Kusch and M.M. Hessel, J. Chem. Phys. 67 (1977) 586; M.M. Hessel and C.R. Vidal, J. Chem. Phys. 70 (1979) 4439; M. Broyer, private communication.

[27] J. Blanc, V. Bonačić-Koutecký, M. Broyer, J. Chevaleyre, Ph. Dugourd, J. Koutecký, C. Scheuch, J.P. Wolf and L. Wöste, J. Chem. Phys. 96 (1992) 1793.

[28] V. Bonačić-Koutecký, M.M. Kappes, P. Fantucci and J. Koutecký, Chem. Phys. Letters 170 (1990) 26.

[29] G.D. Mahan, Many-particle physics, 1st Ed. (Plenum Press, New York, 1981).

[30] D. Tománek and K.H. Bennemann, Surface Sci. 163 (1985) 503; D. Tománek, S. Mukherjee and K.H. Bennemann, Phys. Rev. B 28 (1983) 665; B 29 (1984) 1076 (E); W. Zhong, Y.S. Li and D. Tománek, Phys. Rev. B 44 (1991) 13053.